Magnetic and Geochemical Characterization of the Paleogene Carbonate Sequence in the Tekax Borehole, Yucatan, Mexico

Caracterización magnética y geoquímica de la secuencia carbonatada del Paleógeno en el pozo Tekax, Yucatán, México

Ligia **Pérez-Cruz**[1,2,3,*], Daniel J. **Salomón-Dávila**[1,2], Claudio **Vázquez-Sánchez**[1,2], Alejandro **Ortega-Nieto**[2], Elia J **Escobar-Sánchez**[4], Marysol **Valdés-Hernández**[1,2], Rafael **Venegas-Ferrer**[1], Jaime **Urrutia-Fucugauchi**[1,2]

[1] Programa Universitario de Perforaciones en Océanos y Continentes, Instituto de Geofísica. Universidad Nacional Autónoma de México, Coyoacán 04510, México

[2] Instituto de Investigación Científica y Estudios Avanzados Chicxulub, Parque Científico y Tecnológico de Yucatán, Sierra Papacal, Mérida, Yucatán 97302, Mexico

[3] Coordinación de Plataformas Oceanográficas, Coordinación de la Investigación Científica, Universidad Nacional Autónoma de México, Coyoacán 04510, México

[4] Escuela Nacional de Estudios Superiores, Unidad Mérida, Universidad Nacional Autónoma de México, Mérida, Yucatán 97357, México

* Corresponding author: (L. Pérez Cruz)
perezcruz@igeofisica.unam.mx

How to cite this article:
Pérez-Cruz, L., Salomón-Dávila, D.J, Vázquez-Sánchez, C., Ortega-Nieto, A., Escobar-Sánchez, E.J., Váldes-Hernández, M., Venegas-Ferrer, R., Urrutia-Fucugauchi J., 2024, Magnetic and Geochemical Characterization of the Paleogene Carbonate Sequence in the Tekax Borehole, Yucatan, Mexico: Boletín de la Sociedad Geológica Mexicana, 76 (3), A010324. http://dx.doi.org/10.18268/BSGM2024v76n3a010324

Manuscript received: October 25, 2023
Corrected manuscript received: February 10, 2024
Manuscript accepted: February 28, 2024

Peer Reviewing under the responsibility of Universidad Nacional Autónoma de México.

ABSTRACT

Formation of carbonates involve an interplay of processes, including climate, ocean circulation, marine organisms, sediment sources, transport, deposition and diagenesis. The Yucatan peninsula is characterized by a thick carbonate sequence, which has been studied by geological-geophysical surveys and drilling. Characterizing carbonate systems remains an important yet complex undertaking. Here, results of a magnetic susceptibility and X-ray fluorescence geochemical study are used to characterize the Paleogene carbonate sequence in the Tekax borehole of the Chicxulub Drilling Program. The carbonate sequence is ~222 m thick, formed by limestones, dolomites, carbonate breccias and evaporites. Changes in Si, Ca, Fe, Mg, Al, Ti and magnetic susceptibility correlate with lithology downcore. The Ca contents vary through the sequence with a trend around 24% and low discrete values. The upper unit shows higher Ca contents. The Si contents vary downhole, between about 0.03 to 38 %. The carbonates show weak magnetic susceptibilities associated with diamagnetic and paramagnetic minerals, characteristic of carbonate sediments and reduced terrigenous input. Magnetic hysteresis shows fine grained low coercivity magnetite and titanomagnetites, with PSD and MD domain states. Six units are identified through the lithological column. The carbonate sequence shows effects of varying dissolution, fracturing and dolomitization. The lower carbonate unit above the breccia contact shows evaporites, with gypsum and anhydrites.

Keywords: Chicxulub crater, Tekax borehole, Yucatan peninsula, Paleogene carbonate sequence, Magnetic susceptibility, X-ray fluorescence.

RESUMEN

La formación de secuencias carbonatadas involucra diferentes factores, incluyendo clima, circulación oceánica, organismos, fuentes de sedimentos, transporte, diagénesis y sedimentación. La península de Yucatán se caracteriza por secuencias de carbonatos, estudiadas en proyectos geológico-geofísicos y de perforaciones. La caracterización de carbonatos continúa presentando retos. En este estudio, se analizan los registros de susceptibilidad magnética y geoquímica de fluorescencia de rayos X de la secuencia Paleógena del pozo Tekax, Programa de Perforaciones Chicxulub. La secuencia Tekax está formada por calizas, dolomías, brechas carbonatadas y evaporitas. Los registros de Si, Ca, Fe, Mg, Al y Ti y de susceptibilidad magnética se correlacionan con la litología. El contenido de Ca varía con la profundidad, alrededor de un 24% con valores discretos bajos. La unidad superior muestra contenidos más altos. El contenido de Si varía entre 0.03 y 38%. La susceptibilidad magnética presenta valores bajos diamagnéticos y paramagnéticos, característicos de carbonatos con bajo aporte de terrígenos. Mediciones de histéresis a campos hasta 1.5 T indican minerales de baja coercitividad, posiblemente magnetita y titanomagnetitas con estados de dominio PSD y MD. Se identifican seis unidades en la sección del Paleógeno. La secuencia muestra efectos variables de disolución, fracturamiento y dolomitización. Los sedimentos basales arriba de las brechas de impacto muestran horizontes de evaporitas con yesos y anhidritas.

Palabras clave: Cráter Chicxulub, Pozo Tekax, Península de Yucatán, Secuencia carbonatada del Paleógeno, Susceptibilidad Magnética, Fluorescencia de rayos X

http://dx.doi.org/10.18268/BSGM2024v76n3a010324

1. Introduction

Platform carbonate sequences show complex spatial-temporal distributions, being major components in the geological record. The formation of carbonates involves an interplay of factors including geologic setting, sea-land interactions, climate, bathymetry, ocean circulatiocn, sea level, sediment transport and diagenesis (Burchette and Wright, 1992; Pomar and Hallock, 2008; Reijmer, 2021). The carbonate sequences are major hydrocarbon reservoirs, which include the giant oil fields in the Arabian Peninsula and Gulf of Mexico (Viniegra, 1981; Santiago-Acevedo and Baro, 1992; Bratton *et al.*, 2006). Characterizing carbonate systems remains an important, yet complex undertaking.

In the Gulf of Mexico-Caribbean Sea, a major tectonic element is the Yucatan Block with carbonate sediments deposited over an igneous-metamorphic basement of Pan-African affinity (Marton and Buffler, 1994; Bird *et al.*, 2005; Keppie *et al.*, 2010; Zhao *et al.*, 2020). Scarcity of pre-Cenozoic outcrops has limited the stratigraphic studies, with analyses relaying on borehole data and geophysical models (López-Ramos, 1975). The oil exploration program included geological mapping, gravity surveys and drilling, with the Chicxulub-1, Sacapuc-1 and Yucatan-6 boreholes drilling through >1-1.1 km thick carbonate sediments in northern Yucatan. The boreholes and geophysical logs provide stratigraphic data on the carbonate cover, with intermittent core recovery providing samples of carbonates and the Chicxulub impactite sequence (Hildebrand *et al.*, 1991).

The Cenozoic sedimentation history has been intensively investigated from offshore drilling and geophysical surveys (Galloway *et al.*, 2000). Eustatic and tectonic events and ocean circulation changes

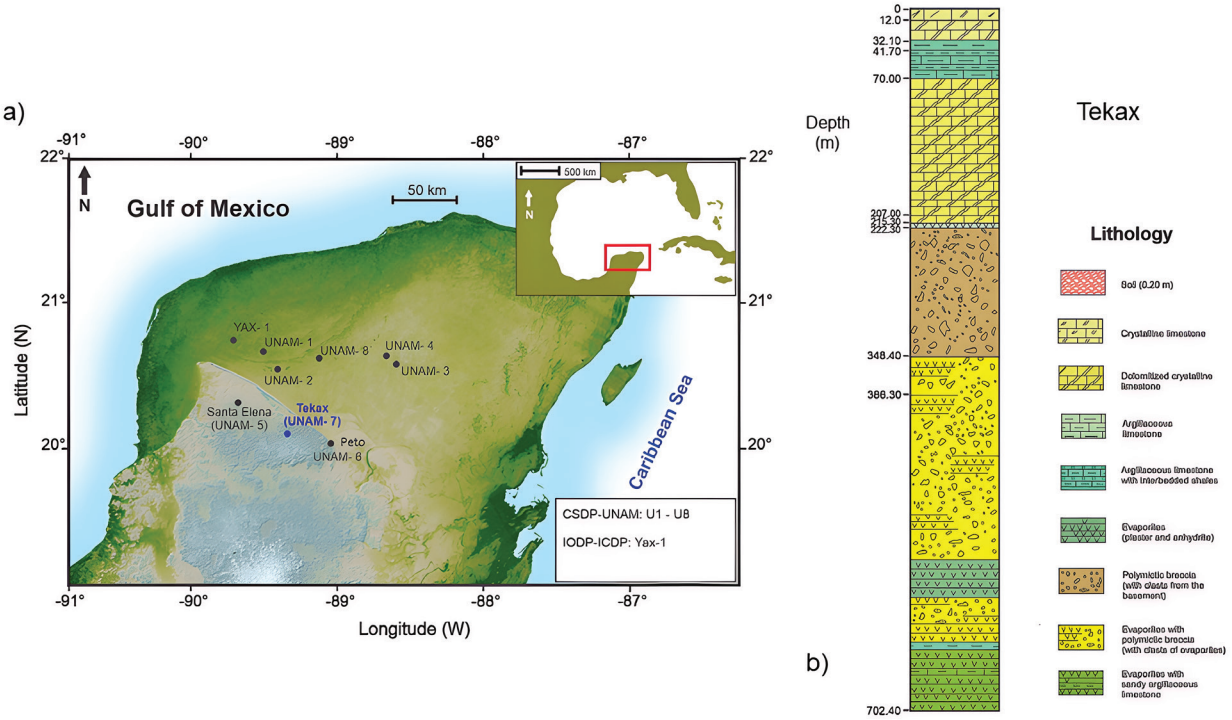

Figure 1 Chicxulub Drilling Program in northern Yucatan. (a) Location of drilling sites with the Tekax borehole in the southern sector. Nearby drilling sites include the Santa Elena and Peto boreholes, which sampled the carbonates and impactites. (b) Schematic column of Tekax borehole with the Paleogene carbonate sequence, impactite breccia sequences (Urrutia-Fucugauchi *et al.*, 1996a, 2011; Rebolledo-Vieyra and Urrutia-Fucugauchi, 2006).

http://dx.doi.org/10.18268/BSGM2024v76n3a010324

have resulted in a complex stratigraphy, with major breaks during the Cretaceous/Paleogene (K/Pg) and the Paleocene-Eocene boundaries recorded (Galloway *et al.*, 2000; Cossey *et al.*, 2016). The ejecta, tsunami, debris flows and collapse deposits associated to the Chicxulub impact provide a regional basin wide stratigraphic marker horizon, which is associated with a major erosive event and regional hiatuses (Denne *et al.*, 2013; Sanford *et al.*, 2016). The impact ejecta has been traced in the Campeche Escarpment, marking a reference horizon in the Yucatan platform (Paull *et al.*, 2014).

The asteroid impact on the Yucatan carbonate platform formed a large ~200 km diameter crater with a complex multiring morphology (Hildebrand *et al.*, 1991, 1998; Sharpton *et al.*, 1992; Schulte *et al.*, 2010). The Chicxulub crater has been investigated with geophysical surveys, modeling and drilling programs (Urrutia-Fucugauchi *et al.*, 2004, 2008, 2011; Collins *et al.*, 2008; Gulick *et al.*, 2013; Doung *et al.*, 2023). The impact formed a depositional basin within the platform that was filled by carbonate sediments, up to 1.1 km in its central sector. The post-impact carbonate sequence provides a high resolution tectonic, paleoclimate and paleoceanographic record, which has been studied as part of the Chicxulub drilling programs with continuous core recovery, which sampled the carbonates and the impactite ejecta (Urrutia-Fucugauchi *et al.*, 1996a, 1996b, 2011). Three boreholes in the southern crater sector, Santa Elena, Peto and Tekax, sampled the impact breccias and the carbonate cover.

The Chicxulub drilling program provided the first continuous lithological columns of the impactite sequence and post-impact sediments. As part of the studies, magnetic susceptibility logging of the Tekax impact breccias documented the inverted stratigraphy with the basement and melt rich breccias on top of the carbonate rich breccias. The upper breccias show high susceptibilities associated with the melt and basement clasts;

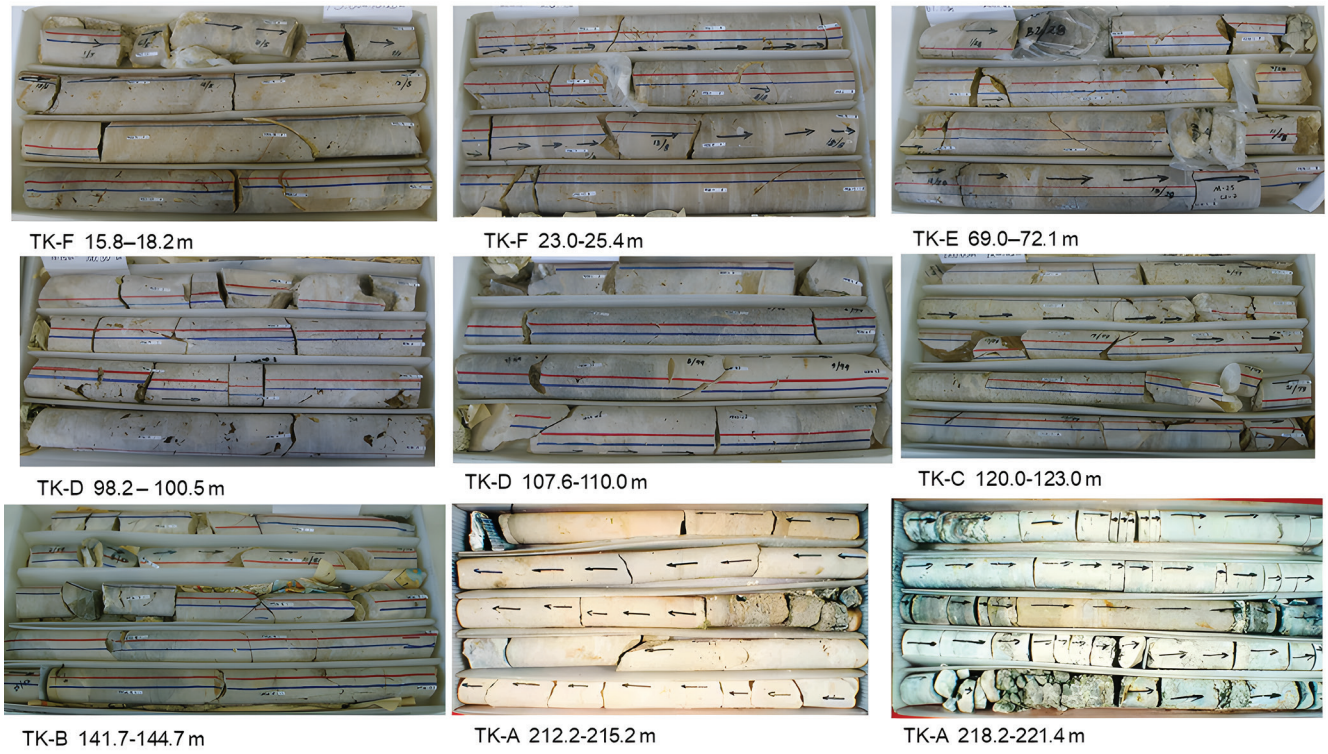

Figure 2 **Tekax borehole cores for the Paleogene carbonates. Core boxes images for intervals through the sequence.**

http://dx.doi.org/10.18268/BSGM2024v76n3a010324

while the lower breccias show low susceptibilities associated with the carbonate clasts and matrix (Urrutia-Fucugauchi *et al.*, 1996a, 1996b, 2014). The inverted ejecta stratigraphy is a characteristic of the ejecta emplacement during collapse of the ejecta plume and lateral curtains.

We present initial results of a rock magnetic and geochemical study of the Paleogene carbonate sequence in the Tekax borehole, which sampled a 222.2 m thick section of carbonates overlying the Chicxulub proximal breccias (Figure 1). In the study we use magnetic susceptibility and x-ray fluorescence (XRF) logging to characterize the sediments. Additionally, we use a staining method to characterize limestones and dolomites, analyzing calcium and magnesium contents and replacement percentages.

1.1. TEKAX BOREHOLE

The Tekax borehole was drilled as part of the Chicxulub drilling program, undertaken to investigate the impactite breccias and melt rocks, the post-impact sediments and the target sequences (Urrutia-Fucugauchi *et al.*, 1996a, 1996b; Rebolledo-Vieyra *et al.*, 2000). The drilling site is located approximately 3.4 km east of the town of Tekax in southern Yucatan (Figure 1a).

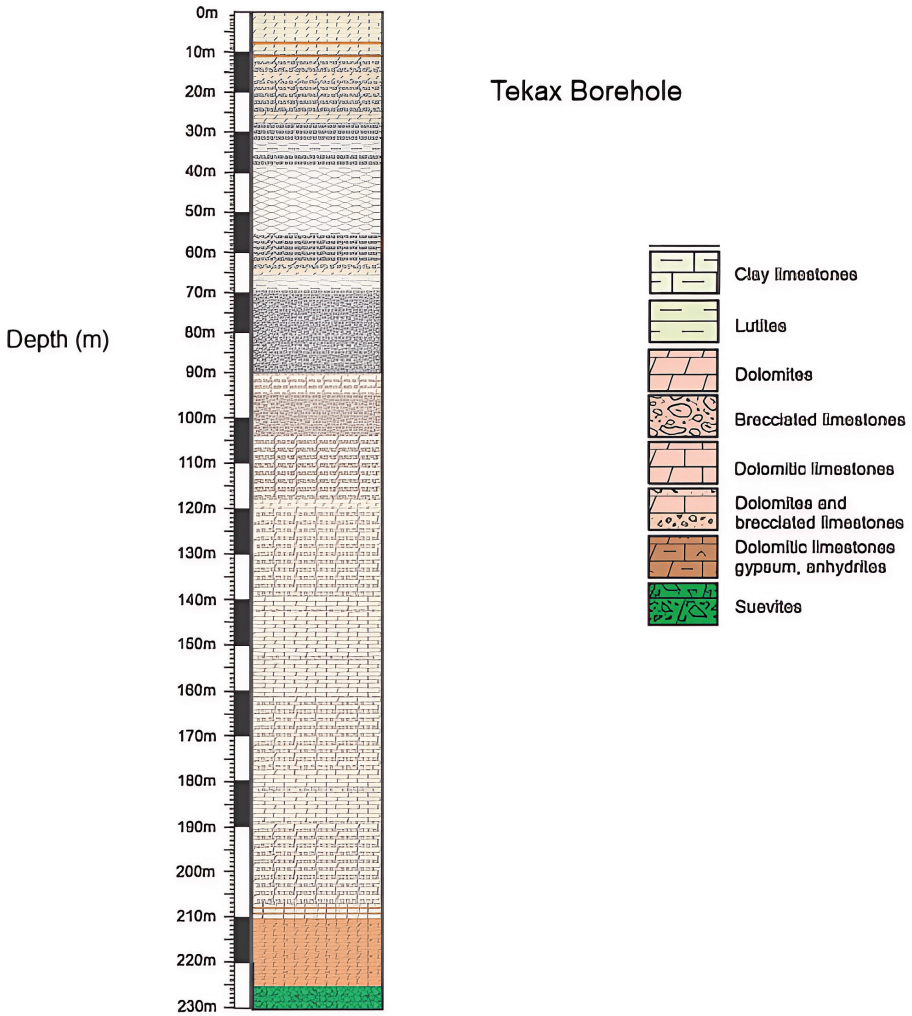

Figure 3 Tekax borehole lithological column for the Paleogene carbonate sequence (Ortega-Nieto, 2014). The interval is from 0 to 222 m depth, above the impact breccia-carbonate contact at 222.1 m.

http://dx.doi.org/10.18268/BSGM2024v76n3a010324

The drilling site lies outside the crater rim as marked by the ring of cenotes (Connors *et al.*, 1996), about 126 m away from the crater center at Chicxulub Puerto, between the gravity rings 3 and 4 identified by Sharpton *et al.* (1993). It is in the southern sector, east of the Ticul fault. Nearby drilling sites include the Ticul, Peto and Santa Elena boreholes (Figure 1).

The Tekax borehole was drilled as part of the Chicxulub drilling program, using a JKS Boyles BBS-37 rig. The maximum drilling depth was 702.4 m, with a core recovery of 651.1 m (Figure 1b), which represents 99% total recovery. The lithological column shows a thin soil layer, the Paleogene carbonate sequence 222.2 m thick and the breccia sequence (Figure 1b). The basal sediments show presence of evaporites and marls, with carbonate breccias. The impactite sequence is formed by upper basement and melt rich breccias and the lower carbonate rich breccias in an inverted stratigraphy. The upper breccia unit was drilled between 222.2 m and 348.4 m and the lower breccias between 348.4 m and 702.4 m (Urrutia-Fucugauchi *et al.*, 1996a).

Paleomagnetic studies of the basal carbonates above the contact with the impact breccias show a reverse polarity for the breccias and normal polarity for the carbonates (Rebolledo-Vieyra and Urrutia-Fucugauchi, 2006). Results for the first 20 m from 224 to 204 m across the contact show five polarity chrons from ch29r to ch27n. The magnetic susceptibility shows a drop from high values in the breccias to low diamagnetic values in the basal carbonates.

The preliminary lithological column was defined from macroscopic analyses of textures, color, fracturing and matrix and clast contents (Figure 2). A study by Ortega-Nieto (2014) based on petrological observations permitted to define the lithological column (Figure 3), which is used in this study.

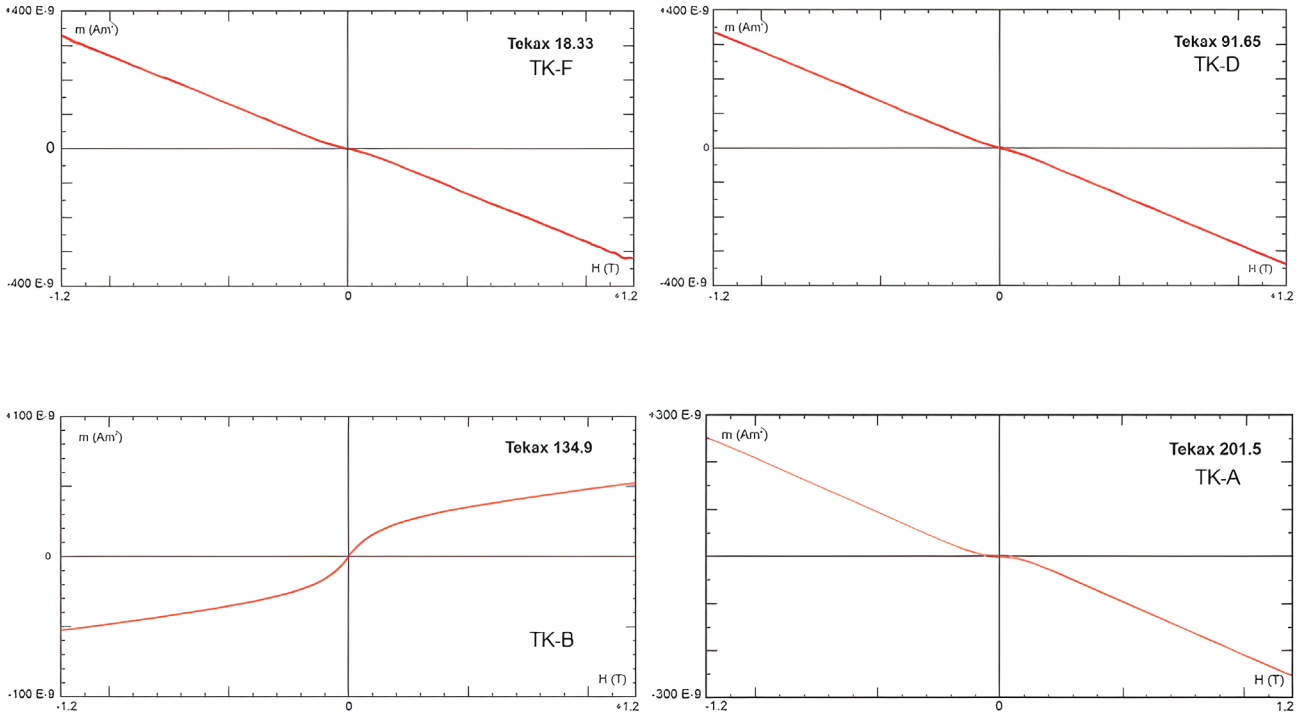

Figure 4 Rock magnetic analyses of the Tekax carbonate sequence. Hysteresis loops before slope correction showing response of the diamagnetic and paramagnetic minerals.

http://dx.doi.org/10.18268/BSGM2024v76n3a010324

2. Methods

The continuous coring with high core recovery rates permits to investigate the lithological column and their changes with depth. Physical property logging and geochemical studies are well suited for characterization of carbonate sediments. Magnetic susceptibility logs have been used to study sedimentary formations and for lateral well correlations (Robinson, 1993; Nowaczyk, 2001; Urrutia-Fucugauchi *et al.*, 2014). X-ray fluorescence analyses on drill core samples provide information on sediment chemical composition, which permits to characterize the drill columns, providing data on the lithology and stratigraphy (Weltjee and Tjalingii, 2008; Hoelzmann *et al.*, 2017; García-Garnica and Pérez-Cruz, 2022).

In this study, we use magnetic susceptibility logging and XRF analyses on the borehole cores. Selection of sampling intervals is based on the macroscopic descriptions, considering changes in lithology, textures, color and degree of fracturing and brecciation (Dunham, 1962; Ortega-Nieto, 2014; Figure 2).

Magnetic susceptibility is a measure of how magnetizable a material is under an applied magnetic field, which varies with the mineralogy and domain state of the magnetic minerals (Dunlop and Ozdemir, 1997). Magnetic susceptibility is a useful parameter for characterizing different lithologies, with a wide range of susceptibilities. The susceptibility depends on mineralogy, size, shape, crystallographic arrangement, and chemical alterations, plus the magnitude of the external field. Rocks with titanomagnetite contents, such as basalts, have higher magnetic susceptibilities than sedimentary rocks with less magnetic minerals, such as limestones.

The susceptibility was measured with a Bartington MS2 meter equipped with the MS2B double frequency sensor with frequencies of 0.465 and 4.65 kHz and calibration accuracy of 1 % (Dearing *et*

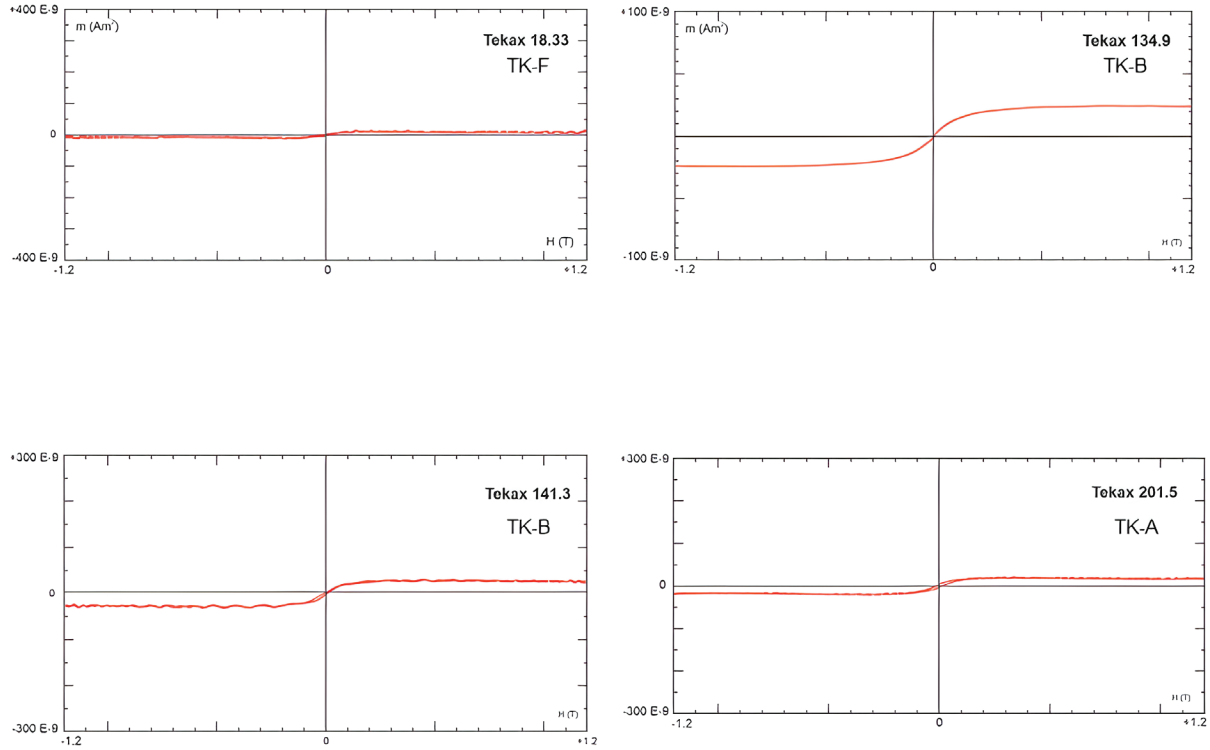

Figure 5 Hysteresis loops after slope correction, showing saturation at low fields.

http://dx.doi.org/10.18268/BSGM2024v76n3a010324

al., 1996). Measurements were taken with spacing around 20 cm.

Further study of the magnetic properties was made measuring the magnetic hysteresis, isothermal remanent magnetization (IRM) acquisition and back field demagnetization of saturation IRM (Dunlop and Ozdemir, 1997). Measurements were done in a MicroMag system, with applied direct fields up to 1.5 T. Analysis of domain state was made using the magnetization-coercivity plot for the ratios of remanent magnetization (Mr) and saturation magnetization (Mrs) as a function of the ratios of remanent (Bcr) and coercivity (Bc). Analysis of domain state for the single domain (SD), pseudo-single domain (PSD) and multi-domain (MD) was done with the ratio plot (Day *et al.*, 1977; Dunlop, 2002).

For the XRF geochemical study, we used the Thermo Scientific Niton XL3t analyzer, which uses a miniaturized 50 kilovolt tube connected to a computer for processing and data storage. A digital imaging scanner records the analyzed surfaces and contact points with the X-ray tube. Measurements are taken in mining mode, with exposure time of 2 minutes. Measurements are taken at 20 cm intervals from 0 to 222 m depth. The XL3t analyzer has been used for semicontinuous analyses in field outcrops and logging cores (*e.g.*, Hoelzmann *et al.*, 2017).

Alizarin red is an organic dye found in orange powder, which has been used in the field and laboratory (Dickson, 1965, 1966). It is diluted in hydrochloric acid to create a staining solution. For this study, 500 ml alizarin red is diluted with 1-2 % HCL in 1-liter distilled water, which allows calcite to react with other carbonates more slowly. Increasing HCL content results in more active effervescence and no staining (Salomon and Vazquez, 2012). The solution will dye the calcite showing a red color. Rock surfaces are washed with distilled water, especially if the rock is microporous, and the staining solution is applied leaving

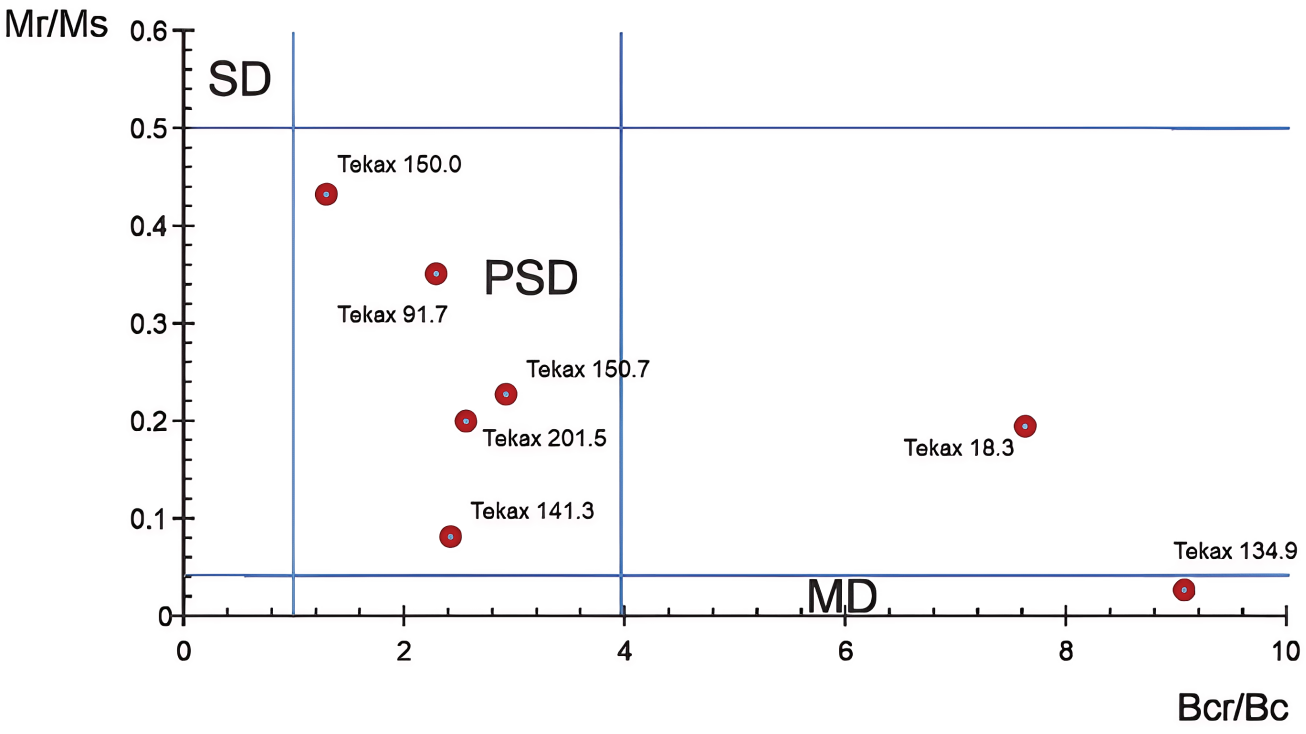

Figure 6 Magnetization-coercivity ratio plot of domain states for the carbonate sequence.

http://dx.doi.org/10.18268/BSGM2024v76n3a010324

it for about 4 minutes. Application of alizarin red solution will show a red dye. The depth, reaction time and the coloration of each sample are recorded. Reaction times were on average 25 s for the calcite (Salomon and Vazquez, 2012).

3. Results

The magnetic susceptibility is characterized by diamagnetic and paramagnetic response, with weak negative and positive susceptibilities. The diamagnetic signal is dominant downcore, correlating with the carbonate lithologies and reduced terrigenous input. The magnetic hysteresis loops show diamagnetic and paramagnetic behavior, with limited ferromagnetic contribution. No contributions of high coercivity minerals are observed. Before slope correction, loops show diamagnetic and paramagnetic loops (Figure 4). After slope correction, the magnetic loops show saturation at small fields, suggesting fine grained titanomagnetites (Figure 5). The IRM acquisition curves show saturation at low fields. In the magnetization-coercivity ratio plot, samples from the different units fall in the PSD field, with some showing MD domain states (Figure 6) The XRF analysis characterizes the chemical elements through the carbonate sequence, characterized by high calcium contents with relatively constant concentrations around 22-26 %. The contents for Ca, Al, K, Fe and Ti are plotted as a function of Si (Figure 5). The Ca-Si diagram shows an inverse relation. The Fe, Al, K, and Ti contents show positive correlations. The Mg contents vary up to 27% (Figure 7). Examples of chemical analyses using the alarzin red hydrochloric acid solution are shown in Figure 8. Fast staining reactions characterize limestones, while low reaction responses indicate dolomitization. The high concentration

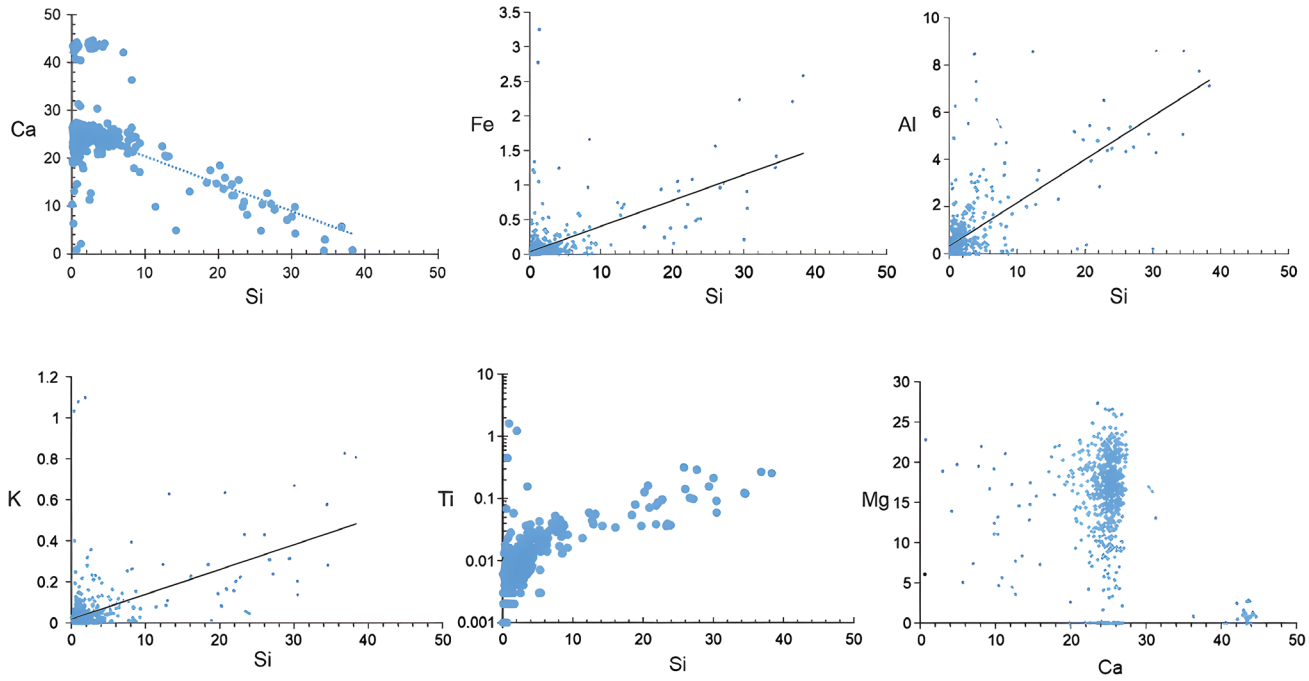

Figure 7 Element plots for XRF analyses of Tekax carbonates for Ca, Fe, Al, K and Ti as a function of Si and Mg as a function of Ca. Regression lines are fitted to the data points.

http://dx.doi.org/10.18268/BSGM2024v76n3a010324

of rapid response is between 50 and 75% (Figure 9). The magnetic susceptibility, geochemical logs and chemical staining analyses document changes in the carbonate sequence downcore (Figures 10 and 11). The Ca contents vary downcore, with a trend around 24% and interspaced discrete low values. The upper sediment unit shows higher Ca contents towards the surface and decreasing downwards. The Si contents vary downhole, from small values up to ~40% and a trend with highs and lows downcore.

4. Interpretation and Discussion

Magnetic susceptibility and geochemical studies are well suited for characterization of carbonate sediments. The initial characterization of the units was based on the core characterization and geochemical logs. The carbonate sequence shows effects of varying dissolution, fracturing and dolomitization. The aluminum, titanium, iron and silica logs show similar trends downhole. The magnetic susceptibility and chemical element log fluctuations correlate with the lithology, with six units defined (Figures 10 and 11).

Unit TK-A (152-222 m) is formed by dolomitic limestones with signs of bioturbation and light gray tones. At ~206 m, lithology changes to consolidated grey-white crystalline limestones with evaporitic nodules of variable sizes from 0.5 cm to 5 cm and fracture. Unit TK-B (130-152 m) is formed by dolomitized limestones and breccias with Si and Fe contents decreasing and variable contents of Al and Mg. Unit TK-C (105-130 m) shows similar lithological characteristics with increase in Si contents and higher Fe contents and magnetic susceptibility. Unit TK-D (72-105 m) is formed by dolomitic breccias with fragments of angular to subangular clasts ranging from 2 mm to 10 cm sizes, supported by light to dark brown dolomite cement. It presents moderate consolidation, with vugular porosities, selective dissolution of cement and fractures. Unit TK-E (28-72m) is

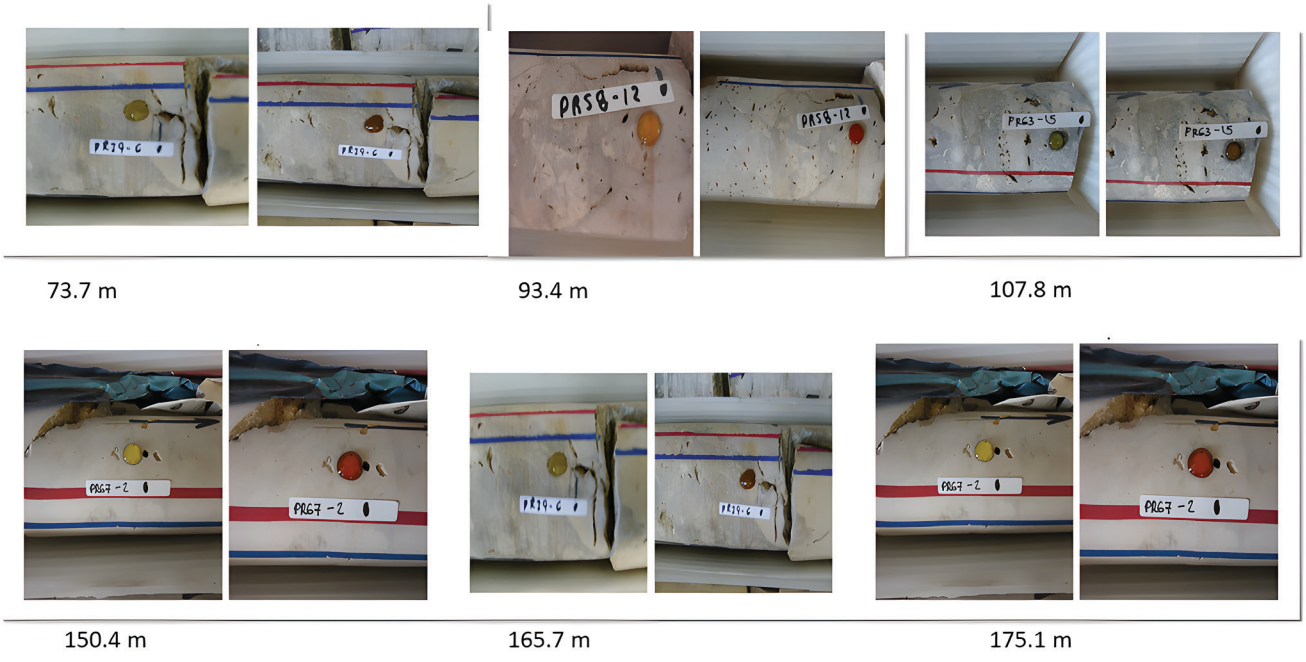

Figure 8 Examples of application of the alarzin red hydrochloric acid solution for cores from different depths through the sequence. Images show the staining reaction.

http://dx.doi.org/10.18268/BSGM2024v76n3a010324

formed by dolomitic breccias, with light brown angular to subangular 0.2-5 cm size clasts in a clayey carbonate matrix of moderate to poor consolidation. Unit TK-F (0-28m) is composed by dolomitized crystalline limestones with cream to light brown tones, below a thin soil cover. It shows ~10-15 cm thick clay horizons with brown-light orange tones. Some parts show limestone clasts in a dolomitized matrix.

The basal sediment section above the impact breccia contact includes evaporites with gypsum and anhydrites from 221 m and decreasing upwards to 210 m. Underlying the evaporites are four meters of smectitic clays. Above the clays, selective dissolution affected the ostracod remains. The magnetic susceptibility shows diamagnetic response, with no indication of hydrothermal alteration or dissolution from the underlying impact breccias.

The hysteresis before slope correction for samples of the basal unit shows a paramagnetic response with a well-defined after slope correction curve (Figures 4 and 5). The basal sediments show evidence of hydrothermal alteration, and it is interesting that the magnetic hysteresis loop before slope correction shows a paramagnetic behavior (Figures 4 and 5). The hysteresis loop after slope correction shows low saturation, likely magnetite or titanomagnetites with higher particle size and MD state (Figure 6). Higher magnetic susceptibilities have been observed at the basal sediments in the Santa Elena and Yaxcopoil-1 boreholes, which have been associated with hydrothermal alteration (Escobar-Sanchez and Urrutia-Fucugauchi, 2010). Analyses of the magnetostratigraphic and stable isotope logs for those boreholes have documented a hiatus at the boundary interval (Urrutia-Fucugauchi and Perez-Cruz, 2008).

The terrigenous input to the sediments in the magnetic susceptibility and chemical logs appears to have been relatively small. The magnetic susceptibility is dominated by diamagnetic and paramagnetic minerals, with reduced terrigenous input and no indication of volcanic material. The circum-Caribbean and Central America magmatic province has been characterized by intense explosive volcanic activity (Sigurdsson *et al.*, 2000; Schindlbeck *et al.*, 2016). Tephra layers have been identified in marine boreholes, which provide a record of volcanic activity in the region. Sigurdsson *et al.* (2000) identified three intervals of explosive activity in the last 55 Ma, during the Paleocene-early Eocene, middle Miocene and Quaternary. Further analyses with high resolution might provide indications of volcanic ash input in his area of the gulf.

Above 178 m depths, we interpret a change from an internal platform environment with presence of grainstone-packstone textures to a sub-

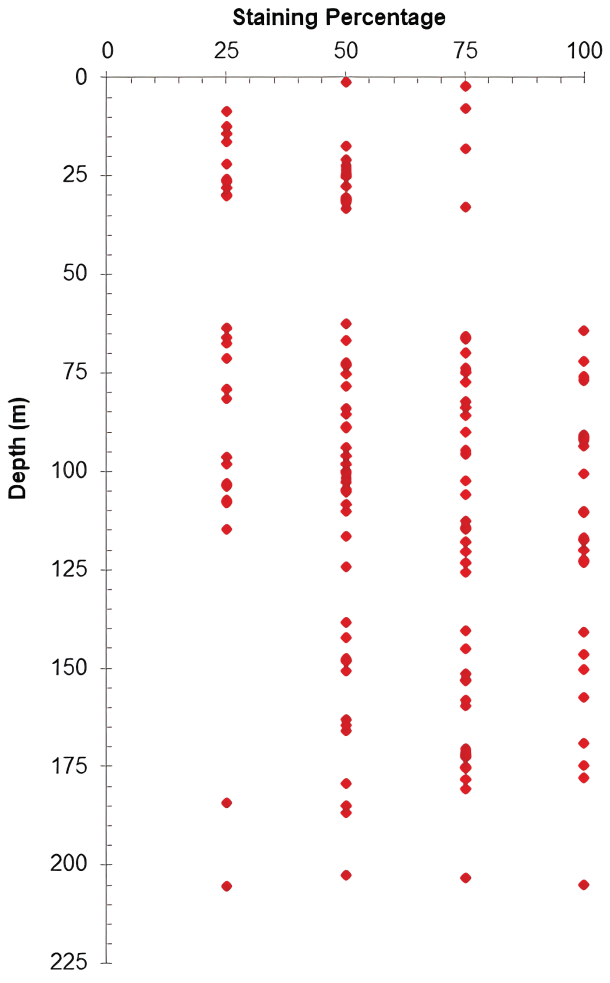

Figure 9 Plot of staining reaction as a function of depth in the carbonate sequence.

http://dx.doi.org/10.18268/BSGM2024v76n3a010324

tidal with the grainstone textures. The downhole changes are associated with eustatic variations. On ramp platforms, mounds are located close to the coastline or lagoon areas (Burchette and Wright, 1992). Towards the section top, dolomitization is intense with an environment of middle internal platform.

In the upper section three units are defined from element concentrations including Ca and Si and the susceptibility log (Figure 10). The Ca shows little variation downcore with contents around 22-26%, except for the TK-F and TK-E sediments, which have higher contents at the surface and decrease downwards to TK-D. Si has low contents less than 10%, with a range up to 38%, with a low wavelength trend with highs and lows downcore for TK-D, TK-C and TK-B units.

The TK-D, TK-C, TK-B and TK-A downcore show small amplitude high frequency changes in Ca content. Units are distinguished by variations in Si, Fe, Ti and magnetic susceptibility (Figure 10, 11). The TK-C unit has higher calcium contents and changes in magnetic susceptibility. The TK-B and TK-A units show similar trends and in the graph they have separated due to a gap in logging. Correlation of logs might constrain the source of Si, which can be from terrigenous or biogenic silica. The silica, aluminum, titanium, and iron logs show similar trends.

The Paleogene carbonates have been cored in the drilling projects, including the Pemex exploratory and the Chicxulub drilling programs (Urrutia-Fucugauchi *et al.*, 1996b, 2004, 2008, 2011; Gulick *et al.*, 2017). The stratigraphy of the

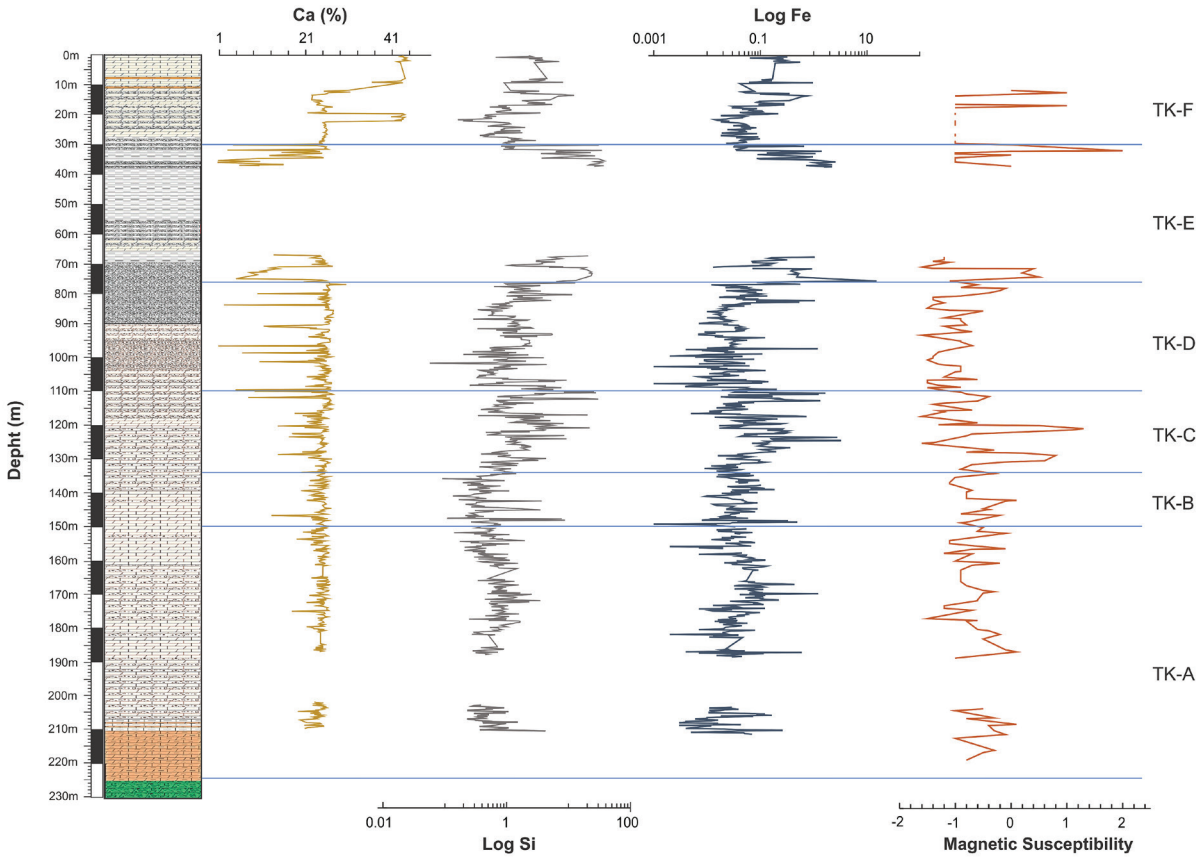

Figure 10 Geochemical logs of the Tekax carbonate sequence for Ca, Si and Fe and the magnetic susceptibility log. For symbols of the lithological column refer to Figure 2. The units TK-A, TK-B, TK-C, TK-D, TK-E and TK-F are indicated.

http://dx.doi.org/10.18268/BSGM2024v76n3a010324

Paleogene sedimentary sequence has been defined from surface geology and borehole correlations (López-Ramos, 1975). Borehole correlations of the Chicxulub drilling program still require further constraints to define the age of sequences. Paleomagnetic and isotope geochemical data are available for the basal units above the breccia-carbonate contact in the Santa Elena, Peto and Tekax and for the Yaxcopoil-1 boreholes (Rebolledo-Vieyra and Urrutia-Fucugauchi, 2004, 2006; Urrutia-Fucugauchi and Perez-Cruz, 2008). Studies of the Paleogene-Eocene thermal maximum and hypothermal events provide additional constrains (Marca-Castillo *et al.*, 2017; Lowery *et al.*, 2021; García-Garnica and Pérez-Cruz, 2022). Marine seismic surveys provide information on the regional stratigraphy, defining stratigraphic packages and regional unconformities that have been correlated to the boreholes (Bell *et al.*, 2004; Whalen *et al.*, 2013; Salguero-Hernandez *et al.*, 2020). Correlations to the M0077A borehole drilled on the crater peak ring of the marine sector provides further constraints (Gulick *et al.*, 2017), yet correlating the M0077A column to the onland boreholes presents uncertainties.

Carbonate deposits constitute important hydrocarbon reservoirs worldwide including the giant and supergiant fields. The study of carbonate deposits presents challenges associated with the characterization of limestones and dolomites, estimates of porosity and permeability, and alteration and deformation effects (Akbar *et al.*, 1995; Bratton *et al.*, 2006). Ahr *et al.* (2005) have analyzed the difficulties in the characterization of carbonate reservoirs and the apparent heterogeneity and classification schemes. Among the difficulties in characterization are the dolomitization and modes of dolomite replacement (Al-Awadi *et al.*,

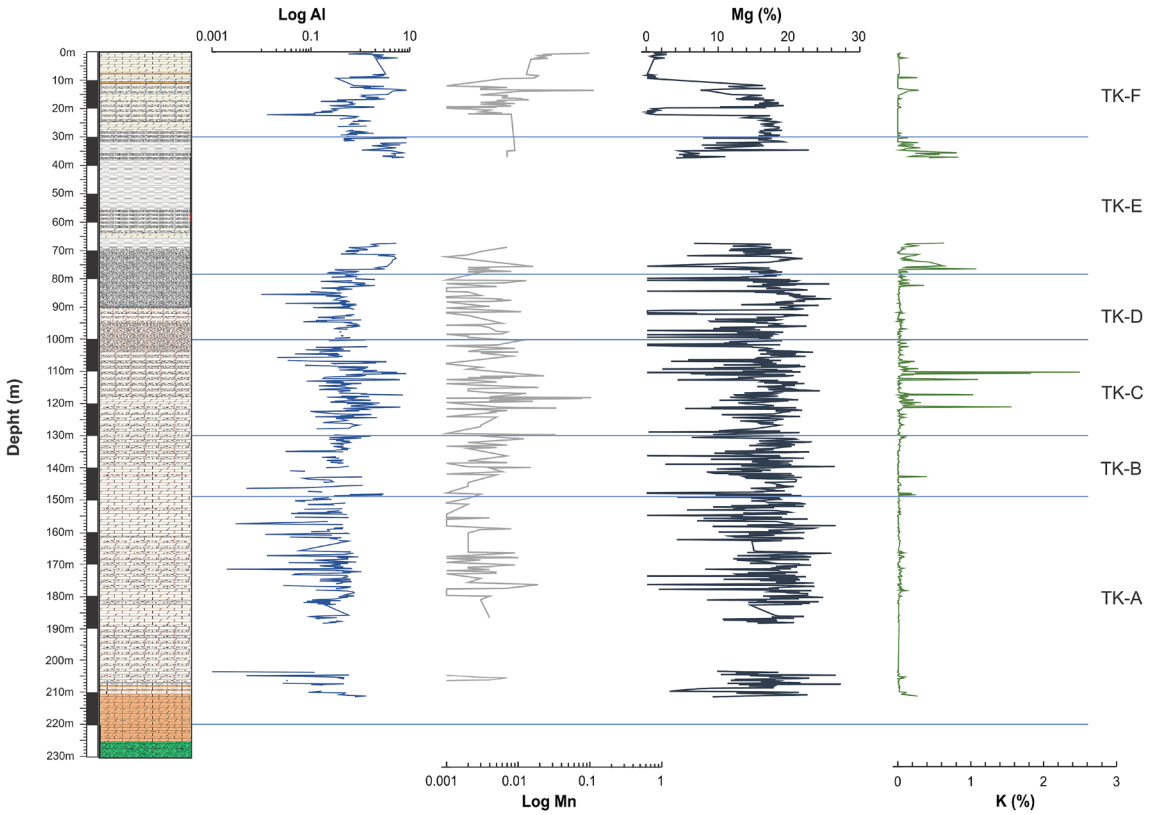

Figure 11 Geochemical logs for Al, Mn, Mg and K. The units TK-A, TK-B, TK-C, TK-D, TK-E and TK-F are indicated.

http://dx.doi.org/10.18268/BSGM2024v76n3a010324

2009), with dolomitization related to porosity in carbonates by replacing Ca ++ ions by Mg ++ ions, reducing the pore volume up to 12 to 13%.

5. Conclusions

XRF geochemical and magnetic susceptibility logging provides a characterization of the Paleogene carbonate sequence in the Tekax borehole, with six carbonate units distinguished downcore.

The carbonates show weak magnetic susceptibilities associated with diamagnetic and paramagnetic minerals, with no input of volcanic ash. Magnetic hysteresis shows fine-grained low-field saturation magnetite and titanomagnetites, with PSD and MD domain states. The hysteresis loops before slope correction are dominated by the diamagnetic signal. The magnetic susceptibility log shows low amplitude fluctuations. The downhole changes in Si, Ca, Fe, Mg, Al and Ti correlate with carbonate lithology, characterizing the column. The Ca contents vary through the sequence with a trend around ~24% and interspaced low discrete values, with the upper unit showing higher Ca contents. The Si contents vary downhole, between about 0.03 to 38%.

Unit TK-A (152-222 m) is formed by dolomitic limestones with signs of bioturbation and light gray tones. At ~206 m, lithology changes to consolidated crystalline limestones with evaporitic nodules of variable sizes and fractures. Unit TK-B (130-152 m) is formed by dolomitized limestones and breccias with Si and Fe contents decreasing and variable contents of Al and Mg. Unit TK-C (105-130 m) shows similar lithological characteristics marked with increase in Si and Fe contents and magnetic susceptibility. Unit TK-D (72-105 m) is formed by dolomitic breccias with fragments of angular to subangular clasts, supported by dolomite cement. Unit TK-E (28-72m) is formed by dolomitic breccias, with angular to subangular clasts in a clay carbonate matrix. Unit TK-F (0-28m) is composed by dolomitized crystalline limestones, with thick clay horizons and dolomitized limestone breccias.

The geochemical and magnetic techniques permit to characterize carbonate sequences in wells with continuous and intermittent core recovery.

Contributions of authors

(1) Conceptualization: LPC, JUF; (2) Analysis: LPC, JUF, DJSD, CVS, AON, EJES, MVH, RVF; (3) Methods: LPC, JUF, DJSD, CVS, AON, EJES, MVH, RVF; (4) Data Acquisition: LPC, JUF, DJSD, CVS, AON, EJES, MVH, RVF; (5) Interpretation: LPC, JUF, DJSD, CVS, AON, EJES, MVH, RVF; (6) Writing: LPC, JUF; (7) Revision: all authors.

Acknowledgements

The study forms part of the Chicxulub Crater Research Program. Thanks to Miguel Angel Díaz and Martin Espinosa for assistance in the laboratory. We acknowledge very useful comments by Dr Manuel Calvo Rathert, an anonymous reviewer and the special volume editor Dr. Daniele Brandt. This is contribution IICEAC 24-005.

Conflict of interest

Authors declare no conflict of interest related to this study.

Handling editor

Daniele Brandt.

References

Ahr, W.M., Allen, D., Boyd, A., Bachman, H.N., Smithson, T., Clerke, E.A., Gzara, K.B.M., Hassall, J.K., Murty, C.R.K., Zubari, H. Ramamoorthy, R., 2005, Confronting the carbonate conundrum: Oilfield Review, 17(1), 18-29.

Al-Awadi, M., Clark, W.J., Moore, W.R., Herron,

M., Zhang, T., Zhao, W., Hurley, N., Kho, D.,Montaron, B., Sadooni, F., 2009, Dolomite: perspectives on a perplexing mineral: Oilfield Review, 21(3), 32-45.

Akbar, M., Petricola, M., Watfa, M., Badri, M., Charara, M., Boyd, A., Cassell, B., Nurmi, R., Delhomme, J.P., Grace, M. Kenyon, B., 1995. Classic interpretation problems: evaluating carbonates. Oilfield Review, 7(1), 38-57.

Bell, C., Morgan, J., Hampson, G.J., Trudgill, B., 2004, Stratigraphic and sedimentological observations from seismic data across the Chicxulub impact basin: Meteoritics and Planetary Science, 39(7), 1089-1098. https://doi.org/10.1111/j.1945-5100.2004.tb01130.x

Bird, D.E., Burke, K., Hall, S.A., Casey, J.F., 2005, Gulf of Mexico tectonic history: Hotspot tracks, crustal boundaries, and early salt distribution. AAPG Bulletin, 89(3), 311-328. https://doi.org/10.1306/10280404026

Bratton, T., Canh, D.V., Van Que, N., Duc, N.V., Gillespie, P., Hunt, D., Li, B., Marcinew, R., Ray, S., Montaron, B. Nelson, R., 2006, The nature of naturally fractured reservoirs: Oilfield Review, 18(2), 4-23.

Burchette, T.P. Wright, V.P., 1992, Carbonate ramp depositional systems: Sedimentary Geology, 79(1-4), 3-57. https://doi.org/10.1016/0037-0738(92)90003-A

Collins, G.S., Morgan, J., Barton, P., Christeson, G.L., Gulick, S., Urrutia-Fucugauchi, J., Warner, M., Wünnemann, K., 2008, Dynamic modeling suggests terrace zone asymmetry in the Chicxulub crater is caused by target heterogeneity: Earth and Planetary Science Letters, 270(3-4), 221-230. https://doi.org/10.1016/j.epsl.2008.03.032

Connors, M., Hildebrand, A.R., Pilkington, M., Ortiz-Aleman, C., Chavez, R.E., Urrutia-Fucugauchi, J., Graniel-Castro, E., Camara-Zi, A., Vasquez, J., Halpenny, J.F., 1996, Yucatan karst features and the size of Chicxulub crater: Geophysical Journal International, 127(3), F11-F14. https://doi.org/10.1111/j.1365-246X.1996.tb04066.x

Cossey, S.P.J., Nieuwenhuise, D. van., Davis, J., Rosenfeld, J.H., Pindell, J., 2016, Compelling evidence from eastern Mexico for a Late Paleocene/Early Eocene isolation, drawdown, and refill of the Gulf of Mexico. Interpretation, 4(1), SC63-SC80. https://doi.org/10.1190/INT-2015-0107.1

Day, R., Fuller, M.D., Schmidt, V.A., 1977, Hysteresis properties of titanomagnetites: grain size and composition dependence: Physics of the Earth and Planetary Interior, 13(4), 260-267. https://doi.org/10.1016/0031-9201(77)90108-X

Dearing, J. A., . Dann, R.J.L., Hay, K., Lees, J.A., Loveland, P.J., Maher, B.A., O'Grady, K., 1996, Frequency-dependent susceptibility measurements of environmental materials: Geophysical Journal International, 124, 228-240. https://doi.org/10.1111/j.1365-246x.1996.tb06366.x

Denne, R.A., Scott, E.D., Eickhoff, D.P., Kaiser, J., Hill, R.J., Spaw, J.M., 2013, Massive Cretaceous-Paleogene boundary deposit, deep-water Gulf of Mexico: New evidence for widespread Chicxulub-induced slope failure: Geology, 41(9), 983–986. https://doi.org/10.1130/G34503.1

Dickson, J.A.D., 1965, A modified staining technique for carbonates in thin section: Nature, 205(4971), 587-587.

Dickson, J.A.D., 1966, Carbonate identification and genesis as revealed by staining: Journal of Sedimentary Research, 36(2), 491-505. https://doi.org/10.1306/74D714F6-2B21-11D7-8648000102C1865D

Duong, T.N.M., Hernawan, B., Medina-Cetina, Z., Urrutia Fucugauchi, J., 2023. Numerical Modeling of an Asteroid Impact on Earth: Matching Field Observations at the Chicxulub Crater Using the Distinct Element Method (DEM): Geosciences, 13(5), 139. https://doi.org/10.3390/geosciences13050139

Dunham, R.J., 1962. Classification of carbonate

http://dx.doi.org/10.18268/BSGM2024v76n3a010324

rocks according to depositional textures, in Ham, W.E., Classification of Carbonate Rocks--A Symposium, AAPG Memoir 1, Tulsa, Oklahoma, American Association of Petroleum Geologists, 108-121.

Dunlop, D.J., 2002, Theory and application of the Day plot (Mrs/Ms versus Hcr/Hc) 1. Theoretical curves and tests using titanomagnetite data: Journal Geophysical Research, Solid earth, 107(B3), https://doi.org/10.1029/2001JB000486

Dunlop, D.J., Özdemir, Ö., 1997, Rock Magnetism: Fundamentals and Frontiers: Cambridge, UK, Cambridge University Press, 573 p.

Escobar-Sanchez, J.E., Urrutia-Fucugauchi, J., 2010, Chicxulub crater post-impact hydrothermal activity-evidence from Paleocene carbonates in the Santa Elena borehole: Geofisica Internacional, 49(2), 97-106. https://doi.org/10.22201/igeof.00167169p.2010.49.2.117

Galloway, W.E., Ganey-Curry, P.E., Li, X., Buffler, R.T., 2000, Cenozoic depositional history of the Gulf of Mexico basin: AAPG Bulletin, 84(11), 1743–1774. https://doi.org/10.1306/8626C37F-173B-11D7-8645000102C1865D

García-Garnica, E.M., Pérez-Cruz, L., 2022, Hyperthermal events recorded in the Palaeogene carbonate sequence of southern Gulf of Mexico—Santa Elena borehole, Yucatan Peninsula: Geological Journal, 57(1), 99-113. https://doi.org/10.1002/gj.4285

Gulick, S.P.S., Christeson, G.L., Barton, P.J., Grieve, R., Morgan, J., Urrutia-Fucugauchi, J., 2013, Geophysical characterization of the Chicxulub impact crater-: Reviews of Geophysics, 51, 31-52. https://doi.org/10.1002/rog.20007

Gulick, S., Morgan, J., Mellett, C.L., Green, S.L., Bralower, T., Chenot, E., Christeson, G., Claeys, P., Cockell, C., Coolen, M., Ferriere, L., Gebhardt, C., Goto, K., Jones, H., Kring, D., Lofi, J., Lowery, C., Ocampo-Torres, R., Perez-Cruz, L., Pickersgill, A.E., Poelchau, M., Rae, A., Rasmussen, C., Rebolledo, M., Riller, U., Sato, H., Smit, J., Tikoo, S., Tomioka, N., Urrutia-Fucugauchi, J., Whalen, M., Wittmann, A., Yamaguchi, K., Xiao, L., Zylberman, W., 2017, Site M0077: Post Impact Sedimentary Rocks, in in Morgan, J., Gulick, S., Mellett, C.L., Green, S.L., and The Expedition 364 Scientists Proceedings of the International Ocean Discovery Program, 364, IODP, 1–35. https://doi.org/10.14379/iodp.proc.364.105.2017

Hildebrand A.R., Penfield G.T., Kring D.A., Pilkington M., Camargo Z., A., Jacbosen S.B. Boynton W.V., 1991, Chicxulub Crater: A possible Cretaceous/Tertiary boundary impact crater on the Yucatán Peninsula, Mexico: Geology, 19(9), .867-871. https://doi.org/10.1130/0091-7613(1991)019<0867:CCAPCT>2.3.CO;2

Hildebrand, A.R., Pilkington, M., Ortiz-Aleman, C., Chavez, R.E., Urrutia-Fucugauchi, J., Connors, M., Graniel-Castro, Camara Zi, A., Halpenny, J.F., Niehaus, D., 1998, Mapping Chicxulub crater structure with gravity and seismic reflection data, in Graddy, M.M., Hutchinson, R., McCall, G.J.H., Rotherby, D.A., (eds.), Meteorites: Flux with Time and Impact Effects: London, Geological Society, London, Special Publications, 140, 155-176. https://doi.org/10.1144/GSL.SP.1998.140.01.12

Hoelzmann, P., Klein, T., Kutz, F., Schütt, B., 2017, A new device to mount portable energy-dispersive X-ray fluorescence spectrometers (p-ED-XRF) for semi-continuous analyses of split (sediment) cores and solid samples: Geoscientific Instrumentation, Methods and Data Systems, 6(1), 93-101.

Keppie, J.D., Dostal, J., Norman, M., Urrutia-Fucugauchi, J., Grajales-Nishimura, M., 2010, Study of melt and a clast of 546 Ma magmatic arc rocks in the 65 Ma Chicxulub bolide breccia, northern Maya block, Mexico:

western limit of Ediacara arc peripheral to northern Gondwana. International Geology Review, 53(10), 1180-1193. https://doi.org/10.1080/00206810903545527

López-Ramos, E., 1975, Geological summary of the Yucatan peninsula, in Nairn, A.E.M., Stehli, F.G. (eds.), The Ocean Basins and Margins, Vol. 3, The Gulf of Mexico and the Caribbean: New York, Plenum, 257-282.

Lowery, C.M., Jones, H.L., Bralower, T.J., Perez-Cruz, L., Gebhardt, C., Whalen, M.T., Chenot, E., Smit, J., Phillips, M.P., Choumiline, K., Arenillas, I., Arz, J.A., García, F., Ferrand, M., Gulick, S.P.S., Expedition 364 Science Party, 2021, Early Paleocene paleoceanography and export productivity in the Chicxulub Crater: Paleoceanography and Paleoclimatology, 36(11), e2021PA004241. https://doi.org/10.1029/2021PA004241

Marca-Castillo, M., Pérez-Cruz, L.L., Urrutia-Fucugauchi, J., 2017, Paleoenvironmental changes during the Paleocene-Eocene recorded in the Yaxcopoil-1 borehole, Chicxulub impact crater: American Geophysical Union Fall Meeting 2017, Abstracts PP23B-1305.

Marton, G., Buffler, R.T., 1994, Jurassic reconstruction of the Gulf of Mexico basin: International Geology Review, 36(6), 545-586. https://doi.org/10.1080/00206819409465475

Nowaczyk, N.R., 2001, Logging of magnetic susceptibility, in Last, W.M., Smol, J.P. (eds.), Tracking Environmental Change Using Lake Sediments. Volume 1: Basin Analysis, Coring, and Chronological Techniques: Dordrecht, The Netherlands, Kluwer Academic Publishers, 155-170.

Ortega-Nieto, A., 2014, Análisis de microfacies en los pozos UNAM-5, 6 y 7 de Yucatán: secuencia carbonatada del Paleoceno – Eoceno: México, UNAM, Programa de Psgrado Ciencias de la Tierra, tesis de Maestría, 132 p.

Paull, C.K., Caress, D.W., Gwiazda, R., Urrutia-Fucugauchi, J., Rebolledo-Vieyra, M., Lundsten, E., Anderson, K., Sumner, E.J., 2014, Cretaceous–Paleogene boundary exposed: Campeche Escarpment, Gulf of Mexico: Marine Geology, 357, 392-400. https://doi.org/10.1016/j.margeo.2014.10.002

Pomar, L., Hallock, P., 2008, Carbonate factories: a conundrum in sedimentary geology: Earth-Science Reviews, 87(3-4), 134-169. https://doi.org/10.1016/j.earscirev.2007.12.002

Rebolledo-Vieyra, M., Urrutia-Fucugauchi, J., 2004, Magnetostratigraphy of the impact breccias and post-impact carbonates from borehole Yaxcopoil-1, Chicxulub impact crater, Yucatán, Mexico: Meteoritics & Planetary Science, 39(6), 821-829. https://doi.org/10.1111/j.1945-5100.2004.tb00932.x

Rebolledo-Vieyra, M., Urrutia-Fucugauchi, J., 2006, Magnetostratigraphy of the Cretaceous/Tertiary boundary and early Paleocene sedimentary sequence from the Chicxulub impact crater: Earth, Planets and Space, 58(10), 1309-1314. https://doi.org/10.1186/BF03352626

Rebolledo-Vieyra, M., Urrutia-Fucugauchi, J., Marin, L.E., Trejo, A., Sharpton, V.L., Soler-Arechalde, A.M., 2000, UNAM scientific shallow-drilling program of the Chicxulub impact crater: International Geology Review, 42(10), 928-940. https://doi.org/10.1080/00206810009465118

Reijmer, J.J.G., 2021, Marine carbonate factories: review and update. Sedimentology, 68(5), 1729-1796. https://doi.org/10.1111/sed.12878

Robinson, S.G., 1993, Lithostratigraphic applications for magnetic susceptibility logging of deep-sea sediment cores: examples from ODP Leg 115, in Hailwood, E.A, Kidd, R.B. (eds), High Resolution Stratigraphy, Geological Society: London, Special Publications, 70(1), 65-98.

http://dx.doi.org/10.18268/BSGM2024v76n3a010324

Salguero-Hernández, E., Pérez-Cruz, L., Urrutia-Fucugauchi, J., 2020, Seismic attribute analysis of Chicxulub impact crater: Acta Geophysica, 68(3), 627-640. https://doi.org/10.1007/s11600-020-00442-z

Salomon, J.D., Vazquez, C., 2012, Métodos no convencionales para caracterización de calizas y dolomías: estudio en la plataforma carbonatada de Yucatán: México, UNAM, Facultad de Ingeniería, tesis Ingenieria Petrolera, 125 p.

Sanford, J.C., Snedden, J.W., Gulick, S.P.S., 2016, The Cretaceous-Paleogene boundary deposit in the Gulf of Mexico: Large-scale oceanic basin response to the Chicxulub impact: Journal Geophysical Research, Solid Earth 121(3), 1240−1261. https://doi.org/10.1002/2015JB012615

Santiago-Acevedo, J., Baro, A., 1992; Mexico's Giant Fields, 1978-1988 Decade Chapter 6, in Giant Oil and Gas Fields of the Decade 1978-1988, AAPG Special Publication A014, 73-99. https://doi.org/10.1306/M54555C6

Schindlbeck, J.C., Kutterolf, S., Freundt, A., Straub, S.M., Vannucchi, P., Alvarado, G., 2016, Late Cenozoic tephrostratigraphy offshore the southern Central America volcanic arc: 2. Implications for magma production rates and subduction erosion: Geochemistry, Geophysics, Geosystems, 17(11), 4585-4604. https://doi.org/10.1002/2016GC006504

Schulte, P., Alegret, L., Arenillas, I., Arz, J.A., Barton, P.J., Bown, P.R., Bralower, T.J., Christeson, G.L., Claeys, P., Cockell, C.S., Collins, G.S., Deutsch, A., Goldin, T.J., Goto, K., Grajales-Nishimura, J.M., Grieve, R.A.F., Gulick, S.P.S., Johnson, K.R., Kiessling, W., Koeberl, C., Kring, D.A., MacLeod, K.G., Matsui, T., Melosh, J., Montanari, A., Morgan, J.V., Neal, C.R., Nichols, D.J., Norris, R.D., Pierazzo, E., Ravizza, G., Rebolledo-Vieyra, M., Reimold, W.U., Robin, E., Salge, T., Speijer, R.P., Sweet, A.R., Urrutia-Fucugauchi, J., Vajda, V., Whalen, M.T., Willumsen. P.S., 2010, The Chicxulub asteroid impact and mass extinction at the Cretaceous-Paleogene boundary: Science, 327(5970), 1214-1218. https://doi.org/10.1126/science.1177265

Sharpton, V.L., Dalrymple, G., Marin, L., Ryder, G., Schuraytz, B., Urrutia-Fucugauchi, J., 1992, New links between the Chicxulub impact structure and the Cretaceous/Tertiary boundary. Nature, 359, 819-821. https://doi.org/10.1038/359819a0

Sharpton, V.L., Burke, K., Camargo-Zanoguera, A., Hall, S., Marin, L., Urrutia-Fucugauchi, J., 1993, Chicxulub multiring impact basin: Size and other characteristics derived from gravity analysis: Science, 261(5128), 1564-1567. https://doi.org/10.1126/science.261.5128.1564

Sigurdsson, H., Kelley, S., Leckie, R.M., Carey, S., Bralower, T., King, J., 2000, History of circum-Caribbean explosive volcanism : Ar/AR dating of tephra layers: Proceedings of the Ocean Drilling Program, Scientific Results, 165, 299-314. https://doi.org/10.2973/odp.proc.sr.165.021.2000

Urrutia-Fucugauchi, J., Pérez-Cruz, L., 2008, Post-impact carbonate deposition in the Chicxulub impact crater region, Yucatan platform, Mexico: Current Science, 95(2), 248-252.

Urrutia-Fucugauchi, J., Marín, L., Trejo, A., 1996a, Initial results of the UNAM scientific drilling program on the Chicxulub impact structure: Rock magnetic properties of UNAM-7 Tekax borehole: Geofísica Internacional, 35(2), 125-133. https://doi.org/10.22201/igeof.00167169p.1996.35.2.854

Urrutia-Fucugauchi, J., Marin, L., Trejo, A., 1996b, UNAM scientific drilling program of Chicxulub impact structure − Evidence for a 300-kilometer crater diameter: Geophysical Research Letters, 23(13), 1565-1568. https://doi.org/10.1029/96GL01566

Urrutia-Fucugauchi, J., Morgan, J., Stoeffler, D. Claeys, P., 2004, The Chicxulub scientific drilling project (CSDP): Meteoritics &

Planetary Science, 39(6), 787-790. https://doi.org/10.1111/j.1945-5100.2004.tb00928.x

Urrutia-Fucugauchi, J., Chavez-Aguirre, J.M., Pérez-Cruz, L., de la Rosa, J.L., 2008, Impact ejecta and carbonate sequence in the eastern sector of Chicxulub crater: Comptes Rendus Geosciences, 340(12), 801-810. https://doi.org/10.1016/j.crte.2008.09.001

Urrutia-Fucugauchi, J., Camargo-Zanoguera, A. Pérez-Cruz, L Pérez-Cruz, G., 2011, The Chicxulub multiring impact crater, Yucatan carbonate platform, Mexico: Geofisica Internacional, 50(1), 99-127. https://doi.org/10.22201/igeof.00167169p.2011.50.1.125

Urrutia-Fucugauchi, J., Pérez-Cruz, L., Campos-Arriola, S.E., Escobar-Sánchez, E., Velasco-Villarreal, M., 2014, Magnetic susceptibility logging of Chicxulub proximal impact breccias in the Santa Elena borehole: implications for emplacement mode: Studia Geophysica et Geodaetica, 58(1), 100-120. https://doi.org/10.1007/s11200-013-0803-0

Viniegra, F., 1981, Great carbonate bank of Yucatan, southern Mexico: Journal of Petroleum Geology, 3(3), 247-278. https://doi.org/10.1111/j.1747-5457.1981.tb00930.x

Weltje, G.J., Tjallingii, R., 2008, Calibration of XRF core scanners for quantitative geochemical logging of sediment cores: theory and application: Earth and Planetary Science Letters, 274(3-4), 423-438. https://doi.org/10.1016/j.epsl.2008.07.054

Whalen, M., Gulick, S., Pearson, Z., Norris, R.D., Pérez-Cruz, L., Urrutia-Fucugauchi, J., 2013, Annealing the Chicxulub impact: Paleogene Yucatan carbonate slope development in the Chicxulub impact basin, Mexico, in Verwer, K., Playton, T.E., Harris, P.M. (eds.), Deposits, Architecture and Controls of Carbonate Margin, Slope and Basinal Settings, Society for Sedimentary Geology Special Publication, 105, 282-304. https://doi.org/10.2110/sepmsp.105.04

Zhao, J., Xiao, L., Gulick, S.P., Morgan, J.V., Kring, D., Urrutia-Fucugauchi, J., Schmieder, M., de Graaff, S.J., Wittmann, A., Ross, C.H., Claeys, Pickersgill, A., Kaskes, P., Goderis, S., Rasmussen, C., Vajda, V., Ferrière, L., Feignon, J.G., Chenot, E., Perez-Cruz, L., Sato, H., Yamaguchi, K., IODP–ICDP Expedition 364 scientists, 2020, Geochemistry, geochronology and petrogenesis of Maya Block granitoids and dykes from the Chicxulub impact crater, Gulf of México: Implications for the assembly of Pangea: Gondwana Research, 82, 128-150. https://doi.org/10.1016/j.gr.2019.12.003